1-1-2012

High-contrast tandem organic light-emitting devices employing semitransparent intermediate layers of LiF/Al/C60

Baofu Ding

Kamal Alameh
Edith Cowan University

10.1021/jp308816w

High contrast tandem organic light emitting devices employing semitransparent intermediate layers of LiF/Al/C60

Bao-Fu Ding, * † Xiao-Yuan Hou, *‡ and Kamal Alameh*†

† Electron Science Research Institute, Edith Cowan University, 270 Joondalup Dr, Joondalup, WA 6027, (Australia).
‡ Key Laboratory of Surface Physics and Key Laboratory of Micro and Nano Photonic Structures (Ministry of Education) Fudan University, Shanghai 200433, (China).

Supporting Information

ABSTRACT: The use of a black cathode with a metal-organic-metal structure is an attractive approach to achieving a high contrast organic light emitting device (OLED) for future-generation flat panel displays. However, the large reduction in OLED power efficiency is currently restricting the use of black cathode for industrial applications. In this paper, a high contrast, high-efficiency tandem OLED employing a black cathode is proposed and experimentally demonstrated. The OLED is implemented by stacking two organic phase tuning layers between a composite intermediate layer of LiF/Al/C_{60} and LiF/Al and optimizing their thicknesses. Electroluminescence spectrum and brightness-current measurement reveal that the phase tuning layer emits photons. Such a tandem device can increase the current efficiency by 110%, and reduce the operating voltage by 1.3 V, in comparison to the conventional high contrast OLED. Measured reflection spectra validate the high-contrast capability of the OLED, and demonstrate experimentally an average reflectance of 5.9 % in the visible range from 400 nm to 750 nm, which is much lower than 20.3% for the conventional high contrast OLED.

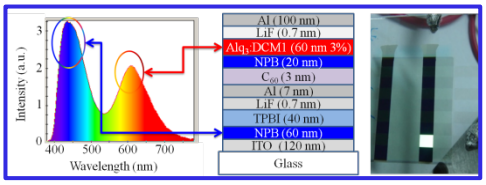

INTRODUCTION

The advantages of organic semiconductors, namely, wide choice of materials, easy fabrication, low cost and transparency, have made organic optoelectronic devices attractive for many applications.[1-6] In particular, organic light emitting diodes (OLEDs) have recently been used for the development of flat panel displays (FPDs) due to (i) their wide viewing angle, (ii) their ultra thin thickness requirements , (iii) their ability to emit light without the need for external backlight sources, (iv) the possibility of growing them on flexible substrates and (v) their low power consumption. In a conventional single-cell OLED, the reflective metal layer benefits the out coupling efficiency of an OLED because the back emission from the organic layer is also reflected forward. Concurrently, such OLEDs have the drawback of low contrast ratio due to the reflection of ambient light by the highly reflective cathode, which degrades the performance of OLEDs especially in outdoor applications where strong ambient light might be present.[3] Recently a black-layer structure is introduced to increase the contrast ratio consisting of a thin semi-transparent metal layer, a phase-tuning (PT) layer made of organic materials and a thick reflective metal layer.[7-9] The low reflection is produced by the cancellation (destructive interference) of two reflected light waves, one from the front thin metal layer and another one with π phase difference with respect to the rear thick metal layer.[9] Due to the simplicity of thermal evaporation methods, organic materials, such as tris8-hydroxyquinoline aluminum (Alq_3) [9,10] and copper phthalocyanine,[11] are the proper candidates for the realization of the PT layer. To obtain the π phase difference, the thickness of organic PT layer must be around 80 nm, which is close to the typical thickness of the emissive layer of OLEDs. Due to the high carrier injection barrier between the PT layer and the intermediate metal layer, the operating voltage more than doubles whereas the current efficiency is reduced by 50%, because the black cathode absorbs half of the generated light emitted by the emissive layer. A two-fold increase in the operating voltage and a 50% reduction in the current efficiency lead to a 75% reduction in the total power efficiency. Such a large reduction in power efficiency undoubtedly restricts its application in industry. In this letter, we study the interface between the intermediate layer and the organic PT layer, and show that the high hole-injecting energy barrier at such interface leads to lower current efficiency and higher operating voltage. Based on the recent discovery that dipole formation between fullerene C_{60} and Al can increase the work function of Al,[12] we propose a high contrast tandem OLED based on inserting an ultrathin C_{60} layer between

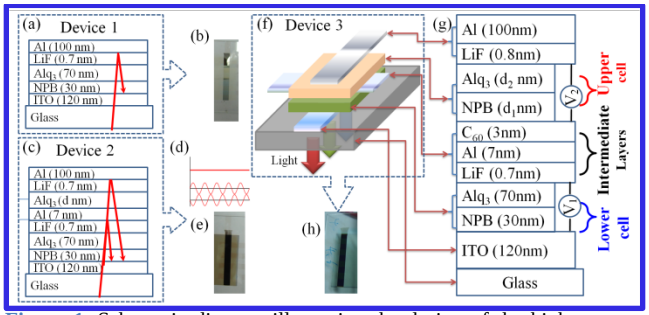

Figure 1. Schematic diagram illustrating the design of the high contrast tandem OLED. (a) The structure and (b) photograph of a conventional single cell OLED (Device 1) illuminated with ambient light. (c) The structure of the single cell OLED with a phase tuning layer (Device 2). (d) Principle of the destructive optical interference (e) Photograph of Device 2 illuminated with ambient light. (f) Schematic diagram, (g) architecture and (h) photograph of the high contrast tandem OLED (Device 3).

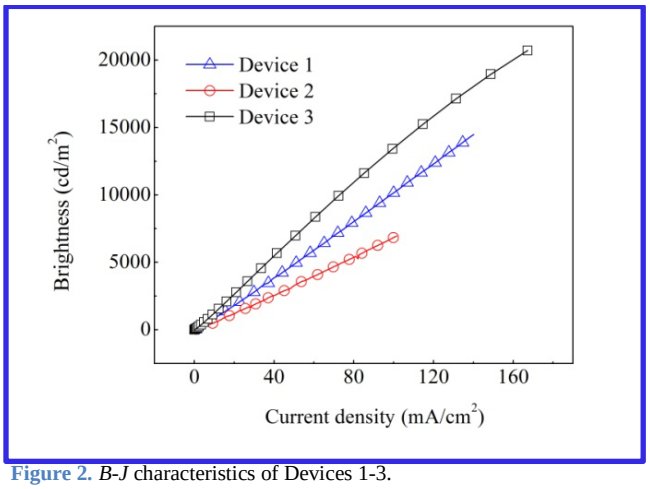

Figure 2. *B-J* characteristics of Devices 1-3.

the intermediate layer of Al and the PT layer, and use electroluminescence (EL) spectral measurements to demonstrate that the PT layer can emit light in addition to its phase-tuning role. The additional role of emitting light from PT layer is prospected to solve the problem of ultralow current efficiency in conventional high-contrast OLEDs. The LiF/Al/C_{60} composite layer can also be used for realizing high-efficiency tandem organic solar cells in future

EXPERIMENTAL METHODS

Device fabrication. The OLED structures were fabricated using thermal sublimation of organic materials in an ultra-high vacuum environment onto transparent glass substrates coated with indium tin oxide (ITO), similar to the process reported in [5,13]. Prior to gas treatment, the procedure for cleaning the substrate included ultrasonication in detergent for 30 minutes, spraying with de-ionized water for 2 minutess, ultrasonication in de ionized water for 20 minutes and drying by rotating at the spinning speed of 2000 rpm in a spin coater for 40 seconds. UV-ozone treatment was then made in a chamber with a high-purity oxygen flow. Immediately after the treatment, the sample was transferred into a growth chamber with a base pressure of 5×10^{-6} Pa for subsequent depositions of various layers. Alq_3 and NPB (N,N′-di(naphthalene-1-yl)-N,N′- diphenylbenzidine were chosen as the electron transporting and emitting layer and the hole transporting layer, respectively, and a top Al layer was chosen as the cathode. TPBI (1,3,5- tris(N-phenylbenzimiazole-2-yl) benzene) was used as an exciton blocking and electron transporting layer. DCM1 (4-(dicyanomethylene)-2-methyl-6-.(p-dimethylaminostyryle) 4H-pyran) is a kind of fluorescent laser dye, which was doped into the host material of Alq_3 to tune the emitting color in this work. To increase the electron injection efficiency, a thin layer of LiF buffer was inserted between the Al and Alq_3 layers, as usually done for conventional OLEDs. The top Al layer had also in the shape of narrow strips, crossing the bottom ITO strips to form active device area of approximately 4×4 mm^2.

EXPERIMENTAL RESULTS AND DISCUSSIONS

3.1. Proposed High Contrast Tandem OLED

Figure 1 illustrates the structures and working principles of three OLEDs, namely (i) a single-cell OLED (Device 1), (ii) a conventional high-contrast OLED (Device 2) and (iii) the proposed high contrast tandem OLED (Device 3). As shown in Figure 1a, for Device 1, two organic layers are sandwiched between a transparent anode of indium tin oxide (ITO) and an almost-fully- reflective back metal layer, such as Al. Ambient light penetrates through the glass substrate/ITO/ Organic layers, and mostly reflects off the thick Al mirror. Therefore, the output light of such an OLED structure results from both the external environment and internal active organic layer. As such, the contrast of this device is very low as shown in Figure 1b. Figure 1c shows the schematic diagram of a conventional high-contrast OLED employing an organic PT layer. Compared to the structure of Device 1, there is an additional metal-organic-metal (MOM) structure on the top of the emissive cell. The LiF (<1 nm)/Al (<8 nm) were used as semitransparent intermediate layers. Ambient light penetrates through the glass substrate and the emissive layer, and partially reflects off the semitransparent intermediate layers. The transmitted light through the latter reflects off the aluminum mirror and interferes with the light reflected off the intermediate layers. The phase difference $\Delta\varphi$ between the two light waves reflected off the upper and lower cells is expressed as:

$$\Delta\varphi = \frac{2n(\lambda)\cdot d}{\lambda} \qquad (1)$$

where n, d and λ are the refractive index, thickness of the PT layer and the wavelength of light, respectively. Factor 2 in the Eq. (1) is due to the round trip of the light wave in the PT layer. By changing d, $\Delta\varphi$ can be varied in the range of 0~π. For $\Delta\varphi$= π, destructive optical interference occurs as illustrated in Figure 1d. The cancellation of the two reflected light beams results in a dark cathode as shown in Figure 1e. Based on the black MOM structure illustrated in Figure 1c, the design of the proposed high contrast tandem OLED, Device 3, is illustrated in Figure 1f and 1g. It consists of an upper cell (coated with a thick aluminum mirror) and a lower cell connected through semi-transparent intermediate nano-layers. Compared to the structure of Device 2, bilayers of C_{60} (3 nm)/NPB (20 nm) are inserted between the intermediate layer of Al and the PT layer of Alq_3. Due to the low work function of composite LiF/Al layers and the high work function of Al/C_{60} layer,[12] the intermediate layers of LiF/Al/C_{60} act as the cathode for the lower cell and the anode for the upper cell, respectively. Thus LiF/Al/C_{60} can be called an anode-cathode layer (ACL). Therefore, while both upper and lower cells emit light, the PT mechanism ensures that the tandem OLED device attains high contrast operation by changing the thickness of NPB/Alq_3 layers in the upper cell.

3.2. EL of the Proposed High Contrast Tandem OLED

Current Efficiency. Figure 2 shows the measured brightness-current density characteristics for the three devices. It is obvious from Figure 2 that the brightness of Device 2 is approximately half of that of Device 1 at a given current density. For instance, at 40 mA/cm^2, the EL of Device 2 is 2400 cd/m^2, compared with 4050 cd/m^2 luminescence for Device 1 at the same current density. Such reduction in luminance for Device 2 is due to the additional MOM black cathode introduced on top of the bottom emissive cell.[9] Almost half of the photons emitted by the bottom emissive layer are reflected by the bottom and top surfaces of the black cathode. Therefore, even if the PT layer thickness is optimized to suppress the reflected light through destructive optical interference, the current efficiency of this OLED structure is limited since half of the generated light is lost by the black cathode. Therefore, the theoretical current efficiency in such black-cathode-based OLEDs is only half of that of Device 1. However, for the proposed Device 3, the EL at the same current density dramatically increases to 5100 cd/m^2, and in comparison with Device 2, the brightness increases by 110%. Interestingly, the EL of Device 3 is even higher than that of Device 1. Our measured results show that besides the bottom cell, the top MOM structure of Device 3 possibly contributes to photon emission as well.

EL spectra. To investigate the impact of C_{60} layer on the emission spectrum generated by the PT layer, the energy bands at the interface between the composite intermediate layer and the PT layer were analyzed. Generally, the hole-injection barrier in this interface is the energy difference between the work function of the composite intermediate layer and the highest occupied molecular orbit (HOMO) which is analogous to the top of the valence band in an inorganic semiconductor. Figure 3 schematically illustrates the energy band diagrams of the interfaces between the composite intermediate layer and PT layer for Device 2 and Device 3. The work function of Al and the HOMO of Alq_3 are respectively 4.3 eV and 5.7 eV,[14] the hole-injection barrier is 1.4 eV, which is high enough to stop hole injection from Al to Alq_3. Although the PT layer of Alq_3 in Device 2 is a fluorescent material, the blockage of hole injection restricts the exciton formation in the PT layer, and consequently makes the PT layer non-emissive. It is important to note that dipole formation between C_{60} and Al has recently been observed by Lee *et al*,[12] which results from the covalent bonds created by charge transfer. The work function of the C_{60} monolayer adsorbed on Al was consequently changed from 4.3 eV to 5.2 eV, making it a suitable anode for organic light-emitting devices [12] and organic solar cells. [15,16] Therefore, for Device 3 the work function of Al/C_{60} and HOMO of NPB are 5.2 eV and 5.4 eV, respectively.[14,17] The hole-injection barrier is 1.4 eV for Device 2 and reduces to 0.2 eV for Device 3. This barrier is low enough for hole injection from the ACL layer to the PT layer. The injected holes pass through the hole-transporting materials of NPB, and are then captured by electrons in the PT layer of Alq_3 to form excitons.[18] The transition of the formed excitons

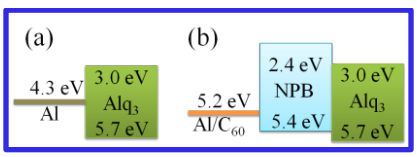

Figure 3. Energy diagrams for (a) Device 2 and (b) Device 3 at the interface between the intermediate layers and the PT layers.

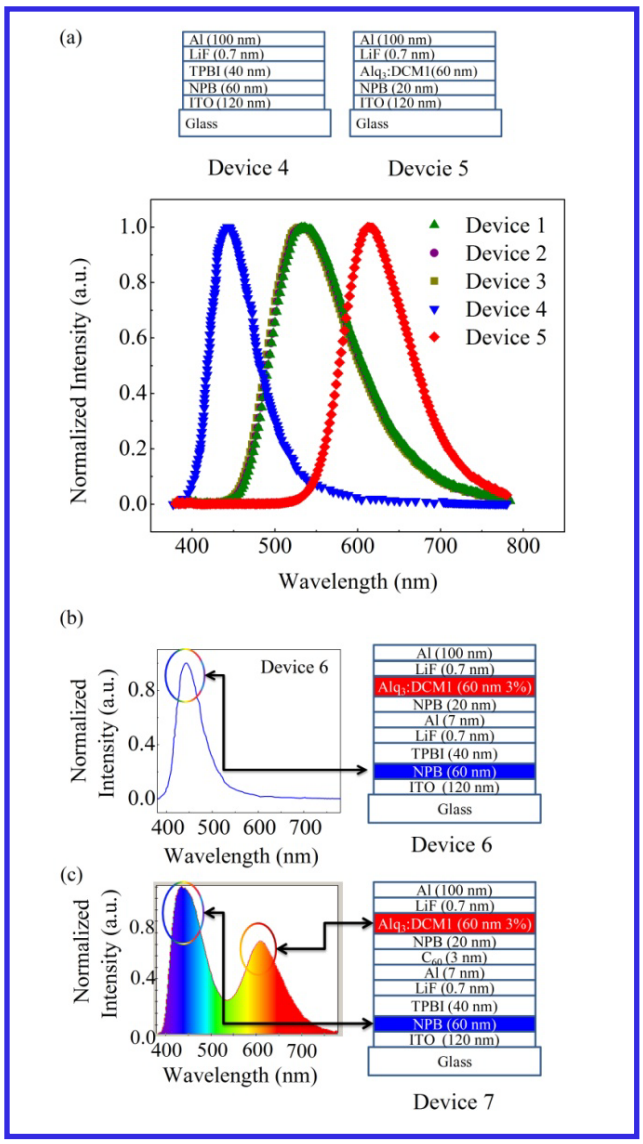

Figure 4. EL spectra for (a) Devices 1-5, (b) Device 6 and (c) Device 7.

yields photon emission from the PT layer. As a result, Device 3 has two emissive cells in tandem, namely, the lower cell and the upper MOM cell. We term the resulting Device 3 as the high contrast tandem OLED.

To directly prove the ACL role of LiF/Al/C_{60}, EL spectrum measurement is employed. Figure 4a shows schematic diagrams of two additional OLED structures, where the Alq_3 layer in Device 1 has been replaced by TPBI and Alq_3:DCM1 as mentioned earlier. The electroluminescence (EL) spectra of Devices 1-5 are also shown in Figure 4a. As seen in Figure 4a the spectra of Devices 1-3 are similar and this is attributed to the fact that their active layers are made of the same Alq_3 material, whose EL spectrum exhibits a peak at around 532 nm. However, for Device 2 or Device 3, both the bottom cell and the PT layer contain Alq_3 materials , making it hard to distinguish which Alq_3 layer emits the the dominant light. To track the light emitting source, we used two different fluorescent materials, whose EL spectra are distinct from each other. For Device 4, NPB was commonly used as the hole transporting material. When inserting an exciton blocking

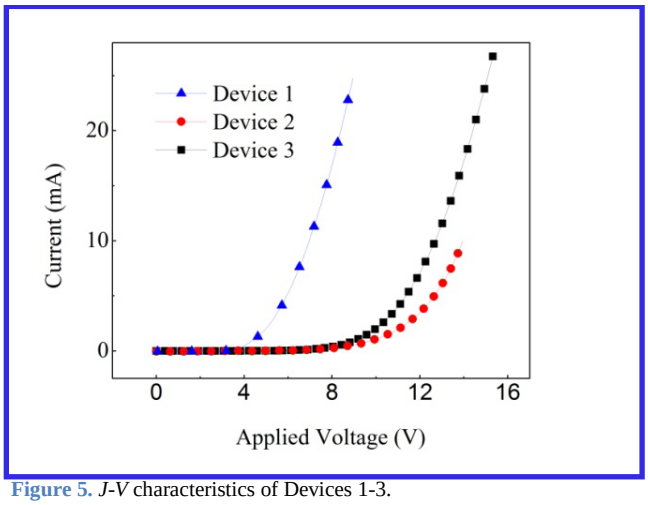

Figure 5. *J-V* characteristics of Devices 1-3.

layer of TPBI between the NPB layer and the cathode in Device 4, excitons were generated and locked inside the NPB layer,[19] and then emitted photons through radiative transition. It is believed that the EL spectrum for Device 4 is mainly generated by the NPB layer. As for Device 5, light emission is known to be generated by the DCM1 material through the "Förster Energy Transfer" and "Charge Trapping" induced by the interaction between the Alq_3 and DCM1 molecules.[20] The EL spectra of Devices 4 and 5 are also shown in Figure 4a, displaying two different peaks around 435 nm and 610 nm and which are in good agreement with the EL spectra of NPB and DCM1 molecules, respectively.[21,22] Based on the results of Figure 4a, two new OLEDs were fabricated, namely, a conventional high-contrast OLED (Device 6) and a high-contrast tandem OLED (Device 7), which are shown in Figure 4b and Figure 4c, respectively, together with their corresponding EL spectra. For Device 6, light emission from only NPB is observed, indicating that the PT layer cannot generates photons, whereas, for Device 7, light emission from both the DCM1 and NPB layers are observed simultaneously, as evident from its two-peak spectrum. Therefore, both the upper cell and the lower cell of Device 7 emit light, implying that the composite LiF/Al/C_{60} layer works as an efficient ACL.

3.3. Operating voltage

Figure 5 shows the *J-V* characteristics for the three devices. At a current of 4 mA, the operating voltage of Device 2 is 12.3 V, almost 7 V higher than that of Device 1. This indicates that the extra 80 nm thick Alq_3 layer introduces a considerably high resistance, resulting in a remarkably higher operating voltage. This is consistent with previous reported results.[23] For Device 3, the operating voltage is 11.0 V, which is 1.3 V lower than that of Device 2. Since the hole injection barrier of the MOM structures for both Device 2 and Device 3 is higher than 0.2 eV, the current flow through the MOM is dominated by the injection limited current (J_{ILC}) as described in Ref. 24, which is expressed as:

$$J_{ILC} = q\mu EN \exp\left(-\frac{q\phi_B}{kT}\right)\exp\left(\frac{q\gamma}{kT}\sqrt{E}\right), \qquad (2)$$

where q is the electron charge, μ is the hole mobility, E is the electric field, N is the density of state, and ϕ_B is the hole injection barrier. From Eq. (2), if ϕ_B is reduced, at a given current, E will also reduce accordingly. With E being proportional to V/L, where V is the operating voltage and L is the thickness of organic layer, the reduction of ϕ_B leads to the reduction of the operating voltage.

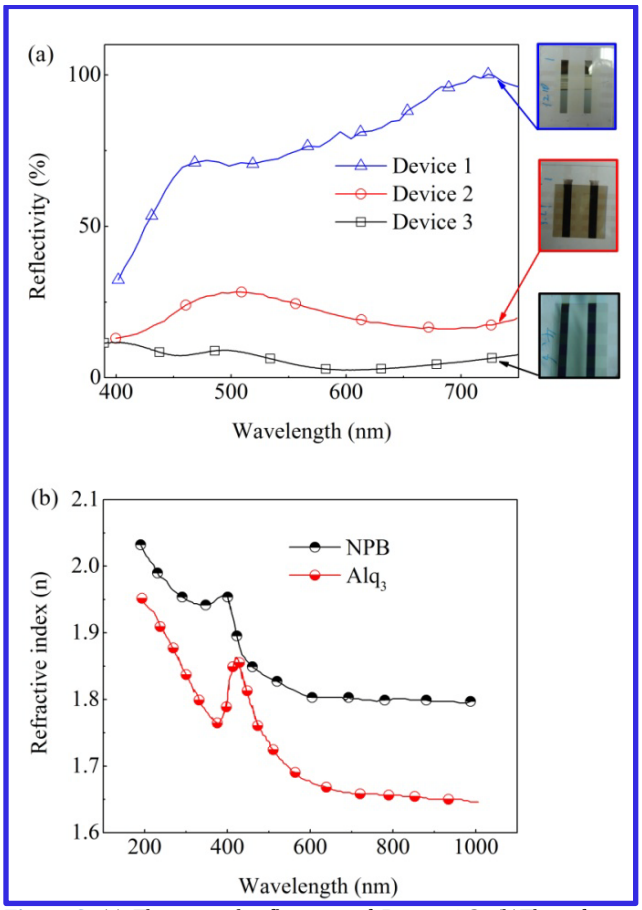

Figure 6. (a) The spectral reflectance of Device 1-3. (b)The refractive indices of NPB and Alq_3.

3.4. Reflectivity

Figure 6a shows the optical reflectance spectra of Devices 1-3 measured at a 5° off the surface normal. The average reflectance of the OLED is 80% for Device 1, 20% for Device 2, mainly due to the addition of the MOM structure. Since there are two PT layers in Device 3, Eq. (1) need to be expanded as :

$$\Delta\varphi = \frac{2\left[n_1(\lambda)\cdot d_1 + n_2(\lambda)\cdot d_2\right]}{\lambda} \qquad (3)$$

where $n_1(\lambda)$ and $n_2(\lambda)$ are the refractive indices of NPB and Alq_3 respectively, and d_1 and d_2 are the thicknesses, of NPB and Alq_3, respectively. To attain maximum destructive interference with the stacked NPB/Alq_3 PT layers in Device 3, the phase difference between the two light waves reflected off the upper and lower cells should be π. Generally, the spectral range of the ambient visible light extends from 400 nm to 750 nm, however, the elimination of the light around 550 nm is the main concern since 550 nm is the most sensitive wavelength to the human eyes. As shown in Figure 6b, at 550 nm, the refractive indices of Alq_3 and NPB are 1.7 and 1.8 respectively. With the NPB thickness being fixed at 20 nm, the optimal Alq_3 thickness is 59 nm, according to Eq. (3). The measured reflectivity from the proposed Device 3 was

only 5.9% over the range of 400 to 750 nm. To our knowledge, this is the lowest reflectance among all high contrast OLEDs based on the use of an organic PT layer. Within the human-eye-sensitive range of 500-600 nm, the reflection value is further reduced to 4%, almost approaching the reflectance of air/glass interface.

CONCLUSIONS

We have proposed the use of a black cathode employing LiF/Al/C_{60} as intermediate semi-transparent layers and NPB/Alq_3 as PT layers to realize a high-contrast and high efficiency OLED. The electroluminescence spectra and bright-current-voltage characteristics for different OLED structures have been investigated, and results have shown that tandem OLED with PT layers can emit light in addition to their role of light phase tuning, opening the way for improving the current efficiency of high contrast OLEDs. An increase of the current efficiency by 120%, a decrease of operating voltage by 1.4 V and a lowered ambient reflectivity of 5.9% over the visible range from 400 nm to 750 nm have been attained in the high contrast tendem OLED, attributed to the photon emission from the PT layer, the reduced carrier injection barrier, between intermediate layer and PT layer, and the proper optical design, respectively. Such big improvements in current efficiency, operating voltage and reflectance make the proposed high contrast tandem OLED much more attractive than conventional high contrast OLEDs for display applications. Moreover, the new developed connecting layer of LiF/Al/C_{60} can have application in other tandem OLED structures and tandem organic solar cells.

AUTHOR INFORMATION

Corresponding Author

* Email:
b.ding@ecu.edu.au;
xyhou@fudan.edu.cn;
k.alameh@ecu.edu.au

ACKNOWLEDGMENT

This research is supported by Edith Cowan University, the Department of Industry, Innovation, Science, Research and Tertiary Education, Australia, and National Natural Foundation, China.

REFERENCES

(1) Friend, R. H.; Gymer, R. W.; Holmes, A. B.; Burroughes, J. H.; Marks, R. N.; Taliani, C.; Bradley, D. D. C.; Dos Santos, D. A.; Bredas, J. L.; Logdlund, M.; Salaneck, W. R. *Nature* **1999**, *397*, 121.

(2) Tang, C. W. *Appl. Phys. Lett.* **1986**, *48*, 183.

(3) Tang, C. W.; Vanslyke, S. A. *Appl. Phys. Lett.* **1987**, *51*, 913.

(4) Dimitrakopoulos, C. D.; Malenfant, P. R. L. *Adv. Mater.* **2002**, *14*, 99.

(5) Ding, B. F.; Zhan, Y. Q.; Sun, Z. Y.; Ding, X. M.; Hou, X. Y.; Wu, Y. Z.; Bergenti, I.; Dediu, V. *Appl. Phys. Lett.* **2008**, *93*, 183307.

(6) Cai, X.; Gerlach, C. P.; Frisbie, C. D. *J. Phys. Chem. C* **2006**, *111*, 452.

(7) Hung, L. S.; Madathil, J. *Adv. Mater.* **2001**, *13*, 1787.

(8) Krasnov, A. N. *Appl. Phys. Lett.* **2002**, *80*, 3853.

(9) Feng, X. D.; Khangura, R.; Lu, Z. H. *Appl. Phys. Lett.* **2004**, *85*, 497.

(10) Zhou, Y. C.; Ma, L. L.; Zhou, J.; Gao, X. D.; Wu, H. R.; Ding, X. M.; Hou, X. Y. *Appl. Phys. Lett.* **2006**, *88*, 233505.

(11) Lee, J. H.; Liao, C. C.; Hu, P. J.; Chang, Y. *Synthetic Met.* **2004**, *144*, 279.

(12) Lee, J. Y. *Appl. Phys. Lett.* **2006**, *88*, 073512.

(13) Ding, B. F.; Yao, Y.; Sun, Z. Y.; Wu, C. Q.; Gao, X. D.; Wang, Z. J.; Ding, X. M.; Choy, W. C. H.; Hou, X. Y. *Appl. Phys. Lett.* **2010**, *97*, 163302.

(14) Ishii, H.; Sugiyama, K.; Ito, E.; Seki, K. *Adv. Mater.* **1999**, *11*, 605.

(15) Wang, M. L.; Song, Q. L.; Wu, H. R.; Ding, B. F.; Gao, X. D.; Sun, X. Y.; Ding, X. M.; Hou, X. Y. *Org. Electron.* **2007**, *8*, 445.

(16) Song, Q. L.; Li, C. M.; Wang, M. L.; Sun, X. Y.; Hou, X. Y. *Appl. Phys. Lett.* **2007**, *90*, 071109.

(17) Cao, J.; Jiang, X. Y.; Zhang, Z. L. *Appl. Phys. Lett.* **2006**, *89*, 252108.

(18) Cheng, Y.-M.; Lu, H.-H.; Jen, T.-H.; Chen, S.-A. *J. Phys. Chem. C* **2010**, *115*, 582.

(19) Wong, K.-T.; Chien, Y.-Y.; Chen, R.-T.; Wang, C.-F.; Lin, Y.-T.; Chiang, H.-H.; Hsieh, P.-Y.; Wu, C.-C.; Chou, C. H.; Su, Y. O.; Lee, G.-H.; Peng, S.-M. *J. Am. Chem. Soc.* **2002**, *124*, 11576.

(20) Ding, B. F.; Yao, Y.; Wu, C. Q.; Hou, X. Y.; Choy, W. C. H. *J. Phys. Chem. C* **2011**, *115*, 20295.

(21) Li, T.; Li, W.; Li, X.; Han, L.; Chu, B.; Li, M.; Hu, Z.; Zhang, Z. *Solid State Electron.* **2009**, *53*, 120.

(22) Gao, X. D.; Zhou, J.; Xie, Z. T.; Ding, B. F.; Qian, Y. C.; Ding, X. M.; Hou, X. Y. *Appl. Phys. Lett.* **2008**, *93*, 083304.

(23) Burrows, P. E.; Bulovic, V.; Forrest, S. R.; Sapochak, L. S.; McCarty, D. M.; Thompson, M. E. *Appl. Phys. Lett.* **1994**, *65*, 2922.

(24) Lee, S. G.; Hattori, R. *Journal of Information Display* **2009**, *10*, 143.